

Article

# Rhodium Nanoparticles Stabilized by PEG-Tagged Imidazolium Salts as Recyclable Catalysts for the Hydrosilylation of Internal Alkynes and the Reduction of Nitroarenes

Guillem Fernández and Roser Pleixats \* 

Department of Chemistry and Centro de Innovación en Química Avanzada (CINQA),  
Universitat Autònoma de Barcelona, 08193 Cerdanyola del Vallès, Barcelona, Spain; guillem.fernandez@uab.cat

\* Correspondence: roser.pleixats@uab.cat; Tel.: +34-93-581-2067

Received: 28 September 2020; Accepted: 12 October 2020; Published: 15 October 2020



**Abstract:** PEGylated imidazolium (bromide and tetrafluoroborate) and tris-imidazolium (bromide) salts containing triazole linkers have been used as stabilizers for the preparation of water-soluble rhodium(0) nanoparticles by reduction of rhodium trichloride with sodium borohydride in water at room temperature. The nanomaterials have been characterized (Transmission Electron Microscopy, Electron Diffraction, X-ray Photoelectron Spectroscopy, Inductively Coupled Plasma-Optical Emission Spectroscopy). They proved to be efficient and recyclable catalysts for the stereoselective hydrosilylation of internal alkynes, in the presence or absence of solvent, and in the reduction of nitroarenes to anilines with ammonia-borane as hydrogen donor in aqueous medium (1:4 tetrahydrofuran/water).

**Keywords:** alkynes; catalysis; hydrosilylation; nitroarenes; recycling; reduction; rhodium nanoparticles

## 1. Introduction

Transition metal nanoparticles (MNPs) as catalysts have received an increasing attention from the chemical community during the last two decades [1–10]. This interest is mainly due to the physical and chemical properties derived from their small size, quantum size effects and high-surface-to volume ratio. Thus, metal nanocatalysts combine the benefits of both homogeneous and heterogeneous catalysis providing high efficiency and selectivity, as well as recyclability. Nanoparticles are thermodynamically unstable and the use of an appropriate stabilizer prevents their agglomeration to bulk metal [11]. Different types of protecting agents have been described (polymers, ionic and non-ionic surfactants, dendrimers,  $\beta$ -cyclodextrins, other ionic compounds, in addition to nitrogen-, sulfur-, and phosphorus-based ligands). The nature and concentration of the protecting shield not only play a role on the activity and selectivity of the nanocatalysts, but also determines their solubility properties. Thus, a suitable choice of the stabilizer allows us the obtention of nanoparticles soluble in organic, fluoruous or aqueous media and facilitates the recycling.

Particularly, both soluble and surface-immobilized rhodium nanoparticles (Rh NPs) have emerged as excellent catalysts with unique properties for hydrogenation reactions and, to a lesser extent, hydroformylation and carbonylation processes [12,13] by a careful design and control of the size/shape of the metallic core and the capping agent [14]. Regarding the hydrogenation reactions, Rh NPs have been mainly used in the reduction of olefins, the aromatic ring of arenes and heteroarenes, and carbonyl compounds. In this work, we have focused our attention on less studied catalytic reactions with Rh NPs, namely selective reduction of nitroarenes to arylamines and hydrosilylation of internal alkynes.

Anilines are useful intermediates for the production of dyes, agrochemicals, fine chemicals, drugs and polymers. Thus, the reduction of nitroarenes [15–17] to anilines is a relevant process in academia and industry. Some encountered issues have to be solved, such as the low chemoselectivity in the presence of other reducible functional groups or the appearance of by-products (hydroxylamines, hydrazines, azoarenes and azoxyarenes) derived from partial reduction of the nitro group and from condensation steps occurring in the reduction process [18]. Catalytic hydrogenation of nitroarenes with dihydrogen has been undertaken with metal nanoparticles (Rh [19], Rh-Fe [20], Au [21,22], Pt [23,24], Pd [25,26], Ni [27,28]). In addition, Rh NPs have also been reported as catalysts for this reduction using hydrazine as hydrogen source [29–32]. Our group has described the catalytic reduction of nitroarenes with Au NPs stabilized by a nitrogen-rich PEG-tagged substrate [33] and with Ni NPs capped by mesitylene-containing tris-imidazolium salts bearing hexadecyl chains [34], using sodium borohydride and hydrazine as reducing agents, respectively.

On the other hand, vinylsilanes are versatile building blocks involved in a range of transformations, such as protodesilylation to give the corresponding alkenes [35], vinyl iodide formation [36], Tamao-Fleming oxidation to provide carbonyl derivatives [37] or Hiyama cross-coupling reactions with vinyl or aryl halides [38]. A convenient and atom-efficient route for the preparation of vinylsilanes is the transition-metal catalyzed hydrosilylation of alkynes [39–44]. Although platinum species (Speier's and Karstedt's catalysts) have been the traditional choice for the addition of silanes to multiple carbon-carbon bonds, other metal complexes have also been investigated. In this context, some reports have appeared on the reaction of both the terminal and internal alkynes with silanes under catalysis by Rh(I) complexes [45–48]; in addition, Rh-NHC species have been used with terminal alkynes [49,50] and molecular Rh(0) complexes confined within carbon nanoreactors have been studied in the hydrosilylation of phenylacetylene [51]. Besides, in the last decade, metal nanoparticles (Pt [52–60], Pd [61,62], Rh-Pt [63], Au [64,65] and Rh [63,66]) have emerged as catalysts for these reactions. In particular, our group has described the catalytic hydrosilylation of internal alkynes with Pd [61] and Pt [60] NPs stabilized by a tris-imidazolium tetrafluoroborate, and with Rh nanoflowers stabilized by a nitrogen-rich polyethylenglicol (PEG)-tagged substrate [66]. As a particular feature, the Pd NPs [61] required anhydrous conditions, because a competitive transfer hydrogenation occurred in the presence of moisture to give the corresponding alkenes and/or alkanes.

Moreover, we have recently reported the obtention of water-soluble gold nanoparticles stabilized by newly designed imidazolium salts bearing PEG-tagged chains (**S1A**, **S1B** and **S2** in Figure 1), which have been found effective recyclable catalysts for the cycloisomerization of  $\gamma$ -alkynoic acids and the  $A^3$  coupling between carbonyl compounds, secondary amines and terminal alkynes [67].

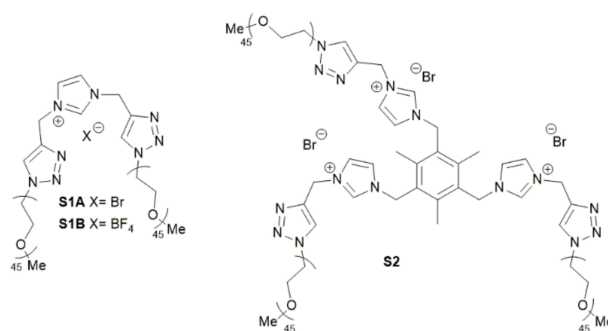


**Figure 1.** PEG-tagged imidazolium salts as stabilizers (previous work: Au NPs; this work: Rh NPs).

Following our interest on the development of soluble metal nanoparticles as recyclable catalysts, we describe herein the preparation and characterization of Rh NPs using these newly synthesized PEG-tagged imidazolium salts as capping agents. Taking into account the scarce precedents on the use of metal NPs for this process (particularly with Rh NPs) and our previous promising results, the hydrosilylation of internal alkynes was one of the catalytic goals that we considered. The second

one was to develop a simple, clean and mild procedure for the chemoselective reduction of nitroarenes to anilines. Thus, we also present here the catalytic activity and recyclability of the Rh NPs for the hydrosilylation of alkynes and the reduction of aromatic nitro compounds.

## 2. Results and Discussion

### 2.1. Preparation and Characterization of Rhodium Nanoparticles

We have prepared rhodium nanoparticles by a chemical reduction of rhodium trichloride hydrate ( $\text{RhCl}_3 \cdot x\text{H}_2\text{O}$ ) with sodium borohydride ( $\text{NaBH}_4$ ) in degassed water ( $\text{H}_2\text{O}$ ) at room temperature in the presence of the corresponding stabilizer **S1A**, **S1B** or **S2** under nitrogen atmosphere (entries 1–3, Table 1). A molar ratio **S**:Rh around 0.02:1 was used, which was found convenient for other type of PEG-tagged ligands [66]. Upon addition of an excess of reducing agent (from 14 to 18 mol per mol of Rh), the reaction mixture changed from orange to blackish. The solution was stirred overnight at room temperature, then it was filtered through a Millipore filter, and the filtrate was extracted with dichloromethane. Upon removal of the solvent, the corresponding nanomaterial was obtained as a black solid, which was stored under inert atmosphere to prevent the oxidation. The obtained Rh NPs were soluble in water, tetrahydrofuran, dichloromethane and chloroform, and insoluble in diethyl ether and hexane.

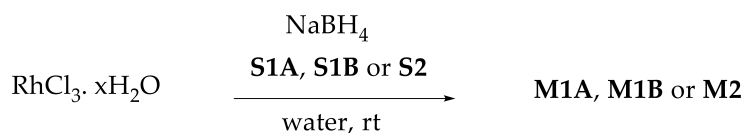


**Table 1.** Preparation of Rh NPs stabilized by **S1A**, **S1B** and **S2**.

Entry	S	S/Rh/ $\text{NaBH}_4$	[Rh] (mM)	Diameter (nm) <sup>1,2</sup>	% Rh		Yield (%) <sup>3</sup>	Nanomaterial
					Theor	Expt		
1	<b>S1A</b>	0.02/1/14	1	$2.9 \pm 3$	30.3	31.7	40	<b>M1A</b>
2	<b>S1B</b>	0.02/1/14	1	$3.3 \pm 2$	30.3	29.9	27	<b>M1B</b>
3	<b>S2</b>	0.025/1/18	0.8	$5.6 \pm 3$	24.2	27.4	41	<b>M2</b>

<sup>1</sup> Determined by TEM (500–1000 particles measured). <sup>2</sup> Larger aggregates of small particles were also formed in entries 2 and 3. See text. <sup>3</sup> Based on  $\text{RhCl}_3 \cdot x\text{H}_2\text{O}$  (40 wt% Rh) used.

Analysis by Transmission Electron Microscopy (TEM) confirmed the formation of small nanoparticles from 2.9 to 5.6 nm, together with flower-like larger aggregates, especially for **M1B** and **M2** (around 33 and 21 nm). These aggregates were smaller (around 14 nm) and less abundant in **M1A** (Table 1 and Figure 2). The tendency to form Rh nanoflowers has been previously observed in the group by decreasing the stabilizer-to-metal ratio [66]. Moreover, the nanoflowers displayed in that case much better catalytic activity than nanomaterials formed by small dispersed nanoparticles.

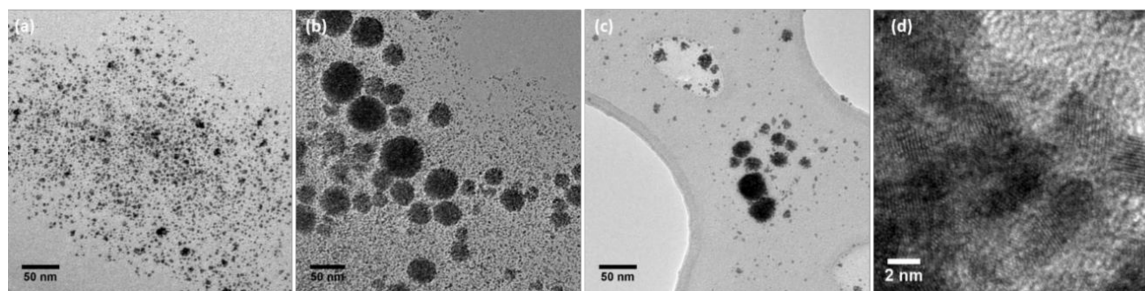


**Figure 2.** TEM images of **M1A** (a), **M1B** (b) and **M2** (c). HRTEM image of **M2** (d).

The presence of rhodium was confirmed by Energy-Dispersive X-ray Spectroscopy (EDS). The spectrum of **M2** is depicted as a representative example in Figure 3.

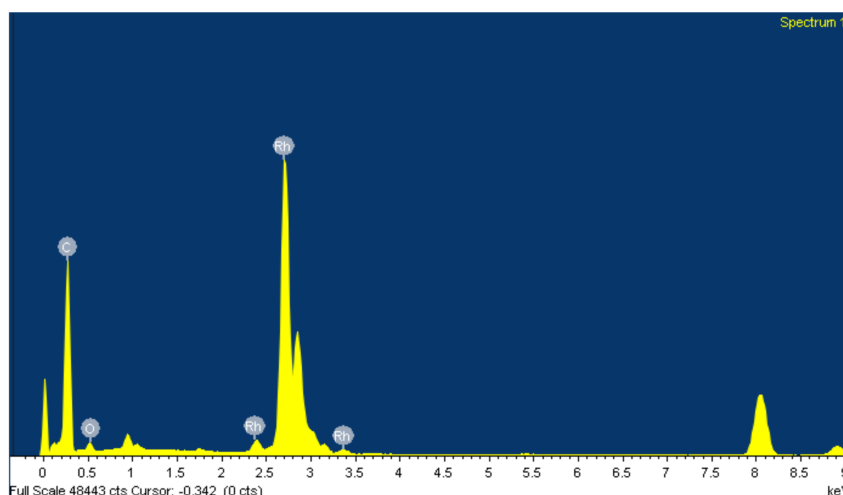


Figure 3. EDS spectrum of M2.

Moderate yields (from 27 to 41%) with respect to the initial amount of rhodium were calculated on the basis of elemental analysis of rhodium in the materials (Inductively Coupled Plasma-Optical Emission Spectroscopy, ICP-OES) (Table 1). The same stabilizers (S1A, S1B and S2) had been found more effective for the formation of gold nanoparticles [67].

High-Resolution Transmission Electron Microscopy (HRTEM) images of M2 (Figure 2d) showed the crystalline planes of the Rh NPs. This was consistent with the Electron Diffraction (ED) analysis, which gave interplanar distances close to those expected for the face-centered cubic (fcc) rhodium lattice (Table 2).

Table 2. Electron diffraction pattern of M2.

hkl	$d_{hkl}$ (nm)	
	Exper.	Theor. <sup>[a]</sup>
(111)	0.2186	0.2196
(200)	0.1907	0.1902
(220)	0.1340	0.1345
(311)	0.1157	0.1147

<sup>[a]</sup> Data according to American Mineralogist Crystal Structure Database.

The nanoparticulated materials M1A, M1B and M2 were analysed by X-ray Photoelectron Spectroscopy (XPS). The doublet at 307.6 and 312.3 eV for Rh 3d<sub>5/2</sub> and Rh 3d<sub>3/2</sub>, respectively (M1B, Figure 4) was attributed to Rh(0) species [68,69]. We did not observe clear peaks at 308.9 and 313.6 eV corresponding to rhodium oxide binding energy [70]. The other nanomaterials (M1A and M2) displayed similar spectra.

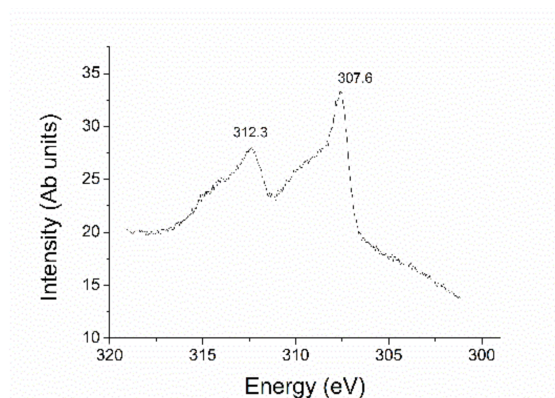


Figure 4. XPS spectrum of M1B.

## 2.2. Hydrosilylation of Alkynes under Catalysis by Rhodium Nanoparticles

With Rh NPs in hand, we undertook the hydrosilylation of a variety of acetylenic compounds. We tested two experimental procedures. In method A the mixture of the alkyne, the catalyst (0.5 mol% Rh loading) and neat silane (4 equiv.) was heated in a sealed vessel at 90 °C [61]. The excess of the volatile silane can be removed easily from the crude mixture. In order to reduce to excess of silane for non-volatile or more expensive silanes, we decided to perform the reaction in a suitable solvent. The use of ethanol did not give successful results, but tetrahydrofuran was found appropriate [60]. Thus, under method B the substrate ( $c = 0.5$  M) was treated with the silane (1.2 equiv.) in tetrahydrofuran (THF) at 90 °C in a closed vessel in the presence of the catalyst (0.5 mol% Rh loading). We summarize in Table 3 the results obtained with three symmetric internal alkynes.

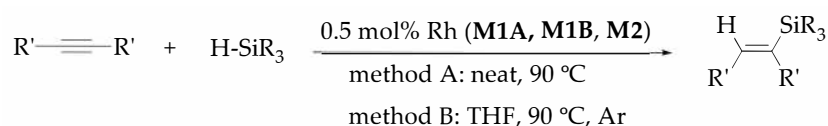


Table 3. Hydrosilylation of symmetric alkynes under catalysis by Rh NPs.

Entry	Catalyst	Product	Method A <sup>1</sup>		Method B <sup>2</sup>	
			Time (h)	Yield (%) <sup>3</sup>	Time (h)	Yield (%) <sup>3</sup>
1	M1A		16	76	24	79
2	M1B		16	84	- <sup>4</sup>	- <sup>4</sup>
3	M2		20	68	- <sup>4</sup>	- <sup>4</sup>
4	M1A		16	84	- <sup>4</sup>	- <sup>4</sup>
5	M1B		16	66	- <sup>4</sup>	- <sup>4</sup>
6	M2		16	78	- <sup>4</sup>	- <sup>4</sup>
7	M1A		16	68	24	97
8	M1B		16	56	- <sup>4</sup>	- <sup>4</sup>
9	M2		- <sup>4</sup>	- <sup>4</sup>	24	90
10	M1A		- <sup>4</sup>	- <sup>4</sup>	24	86

<sup>1</sup> A mixture of alkyne (0.5 mmol), silane (2 mmol) and catalyst (0.5 mol%) was heated a 90 °C in a closed vessel for the given time. <sup>2</sup> A mixture of alkyne (0.5 mmol), silane (0.6 mmol) and catalyst (0.5 mol%) in THF (1 mL) was heated a 90 °C in a closed vessel under argon for the given time. <sup>3</sup> Full conversion in all cases; isolated yields.

<sup>4</sup> Not performed.

Treatment of diphenylacetylene with neat triethylsilane under method A with nanocatalysts M1A, M1B and M2 gave full conversion after heating overnight at 90 °C, affording in a stereoselective way the *syn* addition product **1** (entries 1–3 in Table 3). The same reaction applying the conditions of method B was performed with M1A obtaining similar results after 24 h (entry 1 in Table 3).

In method B, anhydrous THF under argon atmosphere was used in order to avoid the presence of minor amounts of side-products derived from the silane. Under method A, the non-aromatic substrate, 5-decyne, yielded the corresponding vinylsilane **2** (entries 4–6 in Table 3). The reaction of 1,4-dimethoxy-2-butyne with triethylsilane gave the desired product **3** after 16 h under method A and 24 h under method B (entries 7–9 in Table 3). It is worth noting that the same substrate did not produce the vinylsilane **3** under Pt NPs, but the enol ether (*E*)-(1,4-dimethoxy-3-buten-2-yl)triethylsilane [60]. Finally, diphenylacetylene was also made to react with the non-volatile triphenylsilane under conditions B to give the corresponding vinylsilane **4** in 86% isolated yield after 24 h of reaction (entry 10 in Table 3).

Next, the addition of triethylsilane to two asymmetrically substituted diaryl alkynes containing electron-withdrawing (-COCH<sub>3</sub>) and electron-donating (-OMe) groups in *para*-position of one aryl ring was also evaluated using method A (Table 4).

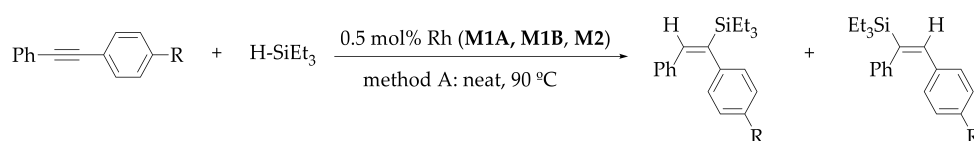


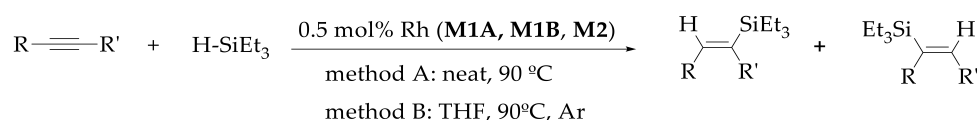
**Table 4.** Hydrosilylation of unsymmetric diaryl alkynes under catalysis by Rh NPs.

Entry <sup>1</sup>	Catalyst	Products	Time (h)	Yield (%) <sup>2</sup>	5:6 <sup>3</sup>
1	M1A		16	98	65:35
2	M1B		16	73	68:32
3	M2	(E)-5a + (E)-6a	16	85	64:36
4	M1A		48	85	43:57
5	M1B		24	97	44:56
6	M2	(E)-5b + (E)-6b	24	92	36:64

<sup>1</sup> A mixture of alkyne (0.5 mmol), silane (2 mmol) and catalyst (0.5 mol%) was heated at 90 °C in a closed vessel for the given time. <sup>2</sup> Full conversion in all cases; isolated yield of the mixture. <sup>3</sup> Molar ratio of the regioisomers determined by nuclear magnetic resonance (NMR) techniques.

Up to four different vinylsilanes could be envisaged with two stereoisomers (*syn*- or *anti*- addition) for each of the two possible regioisomers. As before, a complete stereoselectivity was observed and the reactions afforded the mixtures of the two *syn* regioisomeric vinylsilanes. Higher reaction times were needed for the alkyne bearing the electron-donating group. The regioselectivity was from low to moderate and, in general, did not vary significantly with the different Rh nanocatalysts. The favoured isomer was the one with the triethylsilyl group closest to the more electron-deficient aryl ring, in accordance with the previous results of the group with other nanocatalysts [60,61,66]. The reactions proceeded with lower reaction rates, but with higher regioselectivities than with Pt NPs [60]. By comparison to Pd NPs [61] the regioselectivity was slightly lower and it was quite similar to that observed with other previously reported Rh NPs [66].

Finally, we carried out the hydrosilylation of unsymmetric alkynes presenting two significantly different groups in the two sides of the carbon-carbon triple bond, including two internal and two terminal alkynes, and one 1,3-diyne. In all cases, the silicon reagent involved was triethylsilane (Table 5).

**Table 5.** Hydrosilylation of differentiated unsymmetric alkynes under catalysis by Rh NPs.

Entry	Cat	Products	Method A <sup>1</sup>			Method B <sup>2</sup>		
			t (h)	Yield (%) <sup>3</sup>	7:8 <sup>4</sup>	t (h)	Yield (%) <sup>3</sup>	7:8 <sup>4</sup>
1	M1A		15	69	76:24	24	98	76:24
2	M1B		16	75	77:23	24	94	77:23
3	M2	(E)-7a + (E)-8a	.5	.5	-	24	99	78:22
4	M1A		.5	.5	-	24	80	11:15:74
5	M1B		.5	.5	-	24	85	10:19:71
6	M2	(E)-7b + (E)-8b + (Z)-7b	.5	.5	-	24	79	14:15:71
7	M1A		20	85	65:25:10	.5	.5	-
8	M1B		20	79	59:30:11	.5	.5	-
9	M1A		23	36	80:20	.5	.5	-
10	M1B		23	47	80:20	.5	.5	-
11	M1A	(E)-7c + 8c + (Z)-7c	16	99	-	.5	.5	-
12	M1B		16	64	-	.5	.5	-

<sup>1</sup> A mixture of alkyne (0.5 mmol), silane (2 mmol) and catalyst (0.5 mol%) was heated a 90 °C in a closed vessel for the given time. <sup>2</sup> A mixture of alkyne (0.5 mmol), silane (0.6 mmol) and catalyst (0.5 mol%) in THF (1 mL) was heated a 90 °C in a closed vessel under Ar for the given time. <sup>3</sup> Full conversion in all cases; isolated yields. <sup>4</sup> Molar ratio of the regioisomers determined by NMR techniques. <sup>5</sup> Not performed.

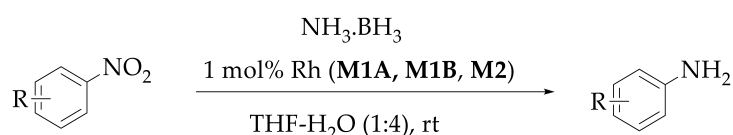
The reaction with propyn-1-yn-1-ylbenzene provided mixtures of the *syn* regioisomers (E)-7a and (E)-8a in about 76:24 molar ratio, which did not change significantly with the nanocatalyst and/or reaction conditions used (entries 1–3, Table 5). Unexpectedly, ethyl 2-butynoate gave as the major isomer (Z)-7b derived from an *anti*-addition process (entries 4–6, Table 5) in sharp contrast with the results previously found with Pt NPs [60] (complete absence of this product) or Pd NPs [61] (minor amount of this isomer). According to the Chalk-Harrod mechanistic cycle [63], an isomerization should take place before the reductive elimination step. The process was regioselective towards the placement of the triethylsilyl group in *gem* to the ester group, in accordance with previous reports on similar  $\alpha$ -directing effect of the electron-withdrawing groups in the hydrosilylation of internal alkynes under platinum [60], palladium [61] or rhodium [66] catalysis.

Then, we performed the reaction with two terminal alkynes, which failed to react with Pd NPs [61]. Phenylacetylene gave rise to the *beta-syn* addition product (E)-7c as main isomer with lower amounts of the *alfa* isomer 8c and the *beta-anti* product (Z)-7c (entries 7–8, Table 5). The reaction of triethylsilane with ethynylcyclohexane exhibited higher selectivity, affording a 80:20 mixture of the corresponding *beta-syn* and *alfa* isomers, (E)-7d and 8d, the *beta-anti* addition compound not being detected (entries 9–10, Table 5). Finally, the hydrosilylation of a symmetrical and sterically crowded 1,3-diyne, such as 2,2,7,7-tetramethylocta-3,5-diyne, was successfully performed under catalysis by



of water) was injected through the septum and the reaction started at room temperature. Complete hydrolysis of AB was accomplished after one hour and about 150 mL of hydrogen were released. The Rh NPs could be recycled up to four runs, although longer reaction times (up to two hours) were needed for complete hydrolysis of AB upon recycling. In the absence of Rh NPs the generation of hydrogen from AB did not occur.

After the demonstration that the nanocatalyst **M2** was effective for the generation of hydrogen from AB, the next step was to find the optimal conditions for the reduction of nitroarenes. The first choice was to carry out the reduction of nitrobenzene (0.5 mmol) with AB (2 mmol) in pure water (10 mL) at room temperature, taking advantage of the solubility of **M2** (used in 1 mol%) in aqueous medium. A fast reaction occurred, after 15 min complete conversion was achieved and aniline was isolated in 92% yield (entry 1, Table 7). The problem arose for nitroarenes less soluble in water, such as *p*-nitrostilbene. Under the same conditions, only 20% conversion was achieved, the precipitation of the substrate preventing further evolution of the reaction. In order to increase to solubility of the substrate, a solution of THF-H<sub>2</sub>O 4:1 (10 mL) was evaluated as reaction medium for *p*-nitrostilbene. In that case, the amount of water was not found enough for complete hydrolysis of AB, reaching just a 50% conversion of the substrate after 18 h. Finally, using a mixture of THF-H<sub>2</sub>O 1:4 (10 mL), the nitro group of *p*-nitrostilbene was completely reduced after 20 h of reaction, achieving the desired *p*-aminostilbene impurified by a small amount of the aniline resulting from the hydrogenation of the olefinic bond (91:9 by <sup>1</sup>HNMR) (entry 2, Table 7).



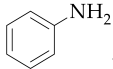
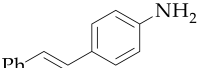
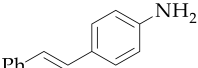
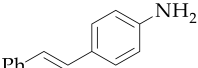
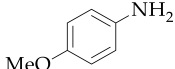
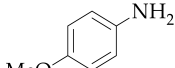
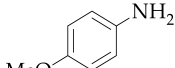
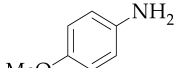
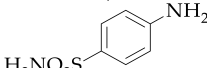
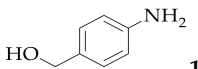
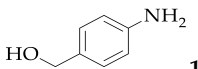
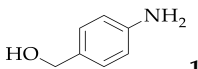
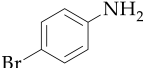
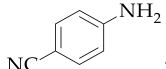
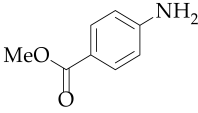
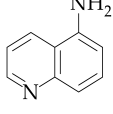
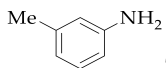
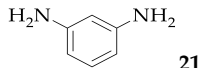
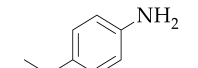
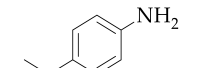
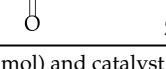
Under these optimized conditions, the reaction scope was then extended to several additional nitroarenes under catalysis by **M1A**, **M1B** and **M2** (Table 7).

The protocol was found to be tolerant to the presence of electron-donating (MeO- in entries 5–8, Me- in entry 17; Table 7) and electron-withdrawing (NH<sub>2</sub>SO<sub>2</sub>- in entry 9, NC- in entry 14, -CO<sub>2</sub>Me in entry 15, Table 7) substituents on the aromatic ring. The cyano and ester groups remained unaltered in the reduction of *p*-nitrobenzotrile (entry 14, Table 7) and methyl *p*-nitrobenzoate (entry 15, Table 7). Also, *p*-bromonitrobenzene furnished *p*-bromoaniline in good yield (entry 13, Table 7), the dehalogenated product being not detected. The heterocyclic compound 5-nitroquinoline gave the 5-quinolinamine **19** in 83% yield after one hour of reaction under **M2** catalysis (entry 16, Table 7). Successful reduction of both nitro groups of *m*-dinitrobenzene was also achieved with **M2**, to afford 1,3-benzenediamine **20** after 2 h of reaction (entry 18, Table 7).

Unfortunately, the reaction was not selective towards the nitro group when an aldehyde function was present. Thus, *p*-nitrobenzaldehyde was reduced to *p*-aminobenzyl alcohol **15** under catalysis by all the Rh nanocatalysts (entries 10–12, Table 7). It is worth to mention that **M1A** provided better selectivity than **M2** for the reduction of *p*-nitrostilbene, affording *p*-aminostilbene as the only product. Conversely, **M1B** was found to be less selective, providing a mixture 85:15 of **11** and **11'** (entries 2–4, Table 7). In the case of *p*-nitroacetophenone, full conversion was achieved in one hour with **M2**, **M1A** and **M1B**, but the desired *p*-aminoacetophenone **22** was accompanied, in all cases, by a small amount of 1-(4-aminophenyl)ethan-1-ol **22'**, arising from the reduction of both the nitro and the carbonyl group (entries 19–21, Table 7).

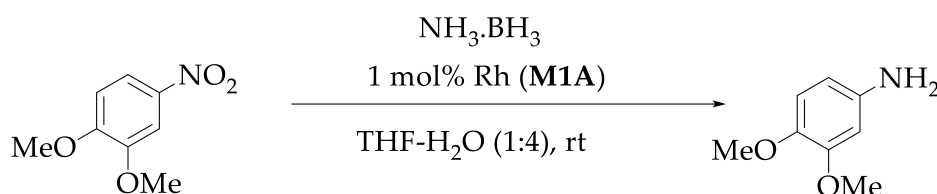
As expected, a blank experiment performed with 3,4-dimethoxynitrobenzene **13** and ammonia borane in the absence of Rh NPs did not give any reduction product after 4 h of reaction.

Table 7. Reduction of nitroarenes with AB under catalysis by Rh NPs.

Entry <sup>1</sup>	Cat.	Product	ArNH <sub>2</sub> /ArNO <sub>2</sub> <sup>2</sup>	Time (h)	Yield (%) <sup>3</sup>
1 <sup>4</sup>	M2		>99:1	0.25	92
2	M2		>99:1	20	91 <sup>5</sup>
3	M1A		>99:1	18	85
4	M1B		>99:1	18	77 <sup>6</sup>
5	M2		>99:1	0.83	81
6	M2		>99:1	0.83	89
7	M1A		>99:1	0.83	92
8	M1B		>99:1	0.83	48
9	M2		>99:1	0.83	58
10	M2		>99:1	1	64
11	M1A		>99:1	1	72
12	M1B		>99:1	1	55
13	M2		>99:1	1	76
14	M2		>99:1	18	85
15	M2		>99:1	1	66
16	M2		>99:1	1	83
17	M2		>99:1	18	53
18	M2		>99:1	2	78
19	M2		>99:1	1	64 <sup>9</sup>
20	M1A		69:31	1	56 <sup>9</sup>
21	M1B		82:18	1	71 <sup>9</sup>

<sup>1</sup> Nitroarene (0.5 mmol), AB (2 mmol) and catalyst (1 mol%) in THF-H<sub>2</sub>O 1:4 (10 mL); rt; in a closed vessel with a balloon. <sup>2</sup> Molar ratio by TLC or <sup>1</sup>H NMR. <sup>3</sup> Isolated yield. <sup>4</sup> Water as solvent. <sup>5</sup> <sup>1</sup>H NMR yield. 4-Phenethylamine **11'** was also obtained. Molar ratio **11:11'** = 91:9. <sup>6</sup> <sup>1</sup>H NMR yield. 4-Phenethylamine **11'** was also obtained. Molar ratio **11:11'** = 85:15. <sup>7</sup> From *p*-nitrobenzaldehyde. <sup>8</sup> From *m*-dinitrobenzene. <sup>9</sup> <sup>1</sup>H NMR yield of the aniline **22**. A minor amount of 1-(4-aminophenyl)ethan-1-ol **22'** was observed.

Taking advantage of the solubility of the rhodium nanocatalysts in water, the recyclability of **M1A** was investigated for the reduction of 3,4-dimethoxynitrobenzene with AB as hydrogen source (Table 8). Five consecutive runs were successfully performed, but longer reactions times were needed for full conversion after the first cycle.

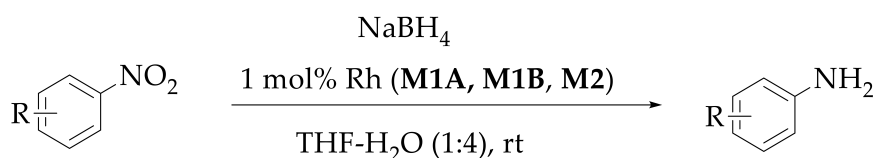


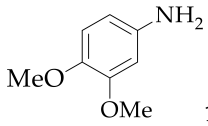
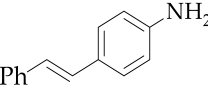
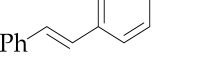
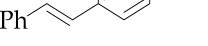
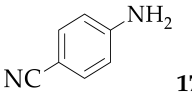
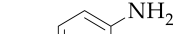
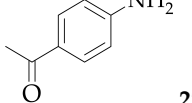
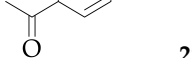
**Table 8.** Recycling of Rh NPs (**M1A**) in the reduction of 3,4-dimethoxynitrobenzene with AB.

Cycle <sup>1</sup>	Time (h)	Yield (%) <sup>2</sup>
1	0.83	92
2	1.25	88
3	18	90
4	18	85
5	24	87

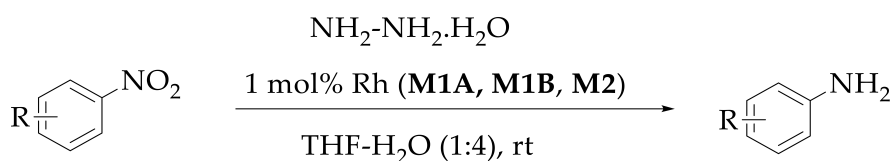
<sup>1</sup> Nitroarene (0.5 mmol), AB (2 mmol) and catalyst (1 mol%) in THF-H<sub>2</sub>O 1:4 (10 mL), rt, in a closed vessel with a balloon. <sup>2</sup> Full conversion in all cases; isolated yield.

With the purpose to overcome the chemoselectivity problems encountered with some substrates, we also assessed the reduction of some nitroarenes using sodium borohydride (NaBH<sub>4</sub>) and hydrazine (NH<sub>2</sub>-NH<sub>2</sub>) as reducing agents. We maintained the other reaction conditions (1 mol% Rh, THF-H<sub>2</sub>O 1:4, rt). We summarize the results in Tables 9 and 10, respectively.

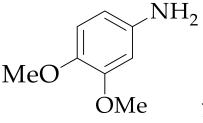
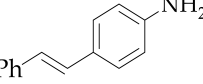
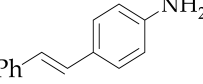
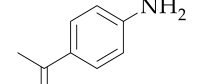
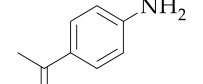
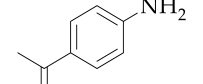
**Table 9.** Reduction of nitroarenes with sodium borohydride under catalysis by Rh NPs.

Entry <sup>1</sup>	Cat.	Product	ArNH <sub>2</sub> /ArNO <sub>2</sub> <sup>2</sup>	Time (h)	Yield (%)
1	<b>M2</b>	 <b>13</b>	>99:1	0.83	66 <sup>3</sup>
2	<b>M2</b>	 <b>11</b>	>99:1	24	77 <sup>4</sup>
3	<b>M1A</b>	 <b>11</b>	>99:1	18	92 <sup>5</sup>
4	<b>M1B</b>	 <b>11</b>	>99:1	18	70 <sup>6</sup>
5	<b>M2</b>	 <b>17</b>	>99:1	18	83 <sup>3</sup>
6	<b>M2</b>	 <b>17</b>	>99:1	0.5	- <sup>7</sup>
7	<b>M1A</b>	 <b>22</b>	69:31	1	58 <sup>8</sup>
8	<b>M1B</b>	 <b>22</b>	>99:1	1	10 <sup>9</sup>

<sup>1</sup> Nitroarene (0.5 mmol), NaBH<sub>4</sub> (2 mmol) and catalyst (1 mol%) in THF-H<sub>2</sub>O 1:4 (10 mL); rt, in a closed vessel with a balloon. <sup>2</sup> Molar ratio by TLC or <sup>1</sup>H NMR. <sup>3</sup> Isolated yield. <sup>4</sup> <sup>1</sup>H NMR yield. 4-Phenethylaniline **11'** was also obtained. Molar ratio **11:11'** = 92:8. <sup>5</sup> <sup>1</sup>H NMR yield. 4-Phenethylaniline **11'** was also obtained. Molar ratio **11:11'** = 97:3. <sup>6</sup> <sup>1</sup>H NMR yield. 4-Phenethylaniline **11'** was also obtained. Molar ratio **11:11'** = 84:16. <sup>7</sup> Not determined, mixture of **22** with 1-(4-aminophenyl)ethan-1-ol **22'** and products derived from the partial reduction of the nitro group. <sup>8</sup> <sup>1</sup>H NMR yield of **22**. Mixture of **22** with 1-(4-aminophenyl)ethan-1-ol **22'**. Molar ratio: 74:26. <sup>9</sup> <sup>1</sup>H NMR yield of the aniline **22**. Mixture of **22** with 1-(4-aminophenyl)ethan-1-ol **22'**. Molar ratio: 36:64.



**Table 10.** Reduction of nitroarenes with hydrazine under catalysis by Rh NPs.

Entry <sup>1</sup>	Cat.	Product	ArNH <sub>2</sub> /ArNO <sub>2</sub> <sup>2</sup>	Time (h)	Yield (%)
1	<b>M2</b>	 <b>13</b>	>99:1	16	70 <sup>3</sup>
2	<b>M1A</b>	 <b>11</b>	62:38	48	48 <sup>4</sup>
3	<b>M1B</b>	 <b>11</b>	29:71	48	23 <sup>4</sup>
4	<b>M2</b>	 <b>22</b>	>99:1	2	- <sup>5</sup>
5	<b>M1A</b>	 <b>22</b>	>99:1	24	- <sup>5</sup>
6	<b>M1B</b>	 <b>22</b>	87:13	24	- <sup>5</sup>

<sup>1</sup> Nitroarene (0.5 mmol), N<sub>2</sub>H<sub>4</sub>·H<sub>2</sub>O (2 mmol) and catalyst (1 mol%) in THF-H<sub>2</sub>O 1:4 (10 mL); rt; in a closed vessel with a balloon. <sup>2</sup> Molar ratio by TLC or <sup>1</sup>H NMR. <sup>3</sup> Isolated yield. <sup>4</sup> <sup>1</sup>H NMR yield. <sup>5</sup> Not determined, mixture of the aniline **22** with other products derived from partial reduction of the nitro group.

The reduction of 3,4-dimethoxynitrobenzene and *p*-nitrobenzoxynitrile with NaBH<sub>4</sub> to the corresponding anilines **13** and **17** proceeded well with **M2**, obtaining similar results as for ammonia borane (entries 1 and 5 of Table 9). However, in the reduction of 4-nitrostilbene under catalysis by **M1A**, **M1B** and **M2**, certain amounts of 4-phenethylamine **11'** were also formed, arising from the reduction of both nitro and olefin groups (entries 2–4, Table 9). As expected, also the carbonyl group of *p*-nitroacetophenone was partially reduced with this reducing agent, affording mixtures of anilines **22** and **22'** in variable proportions depending on the catalyst (entries 6–8, Table 9). For **M2**, complete conversion of the substrate was observed after 30 min, but the analysis of the mixture also revealed the presence of products derived from the partial reduction of the nitro group. In summary, sodium borohydride was not found a better alternative to ammonia borane for the selective reduction of nitroarenes.

Longer reaction times were required for the full reduction of nitroarenes with hydrazine hydrate (NH<sub>2</sub>-NH<sub>2</sub>·H<sub>2</sub>O) under these conditions, in comparison with the previously mentioned reducing agents. However, a 70% isolated yield of the aniline **13** was obtained after 18 h at room temperature (entry 1, Table 10). An increase of the temperature would be needed to accelerate the process. The reaction with *p*-nitrostilbene was sluggish and from low to moderate conversions were obtained after 48 h with **M1B** and **M1A** (entries 2 and 3, Table 10). Nanocatalyst **M2** provided full conversion of *p*-nitroacetophenone after 2 h, but a complex mixture of the aniline **22** and several products derived from the partial reduction of the nitro group was obtained (entry 4, Table 10). The reductions of the same substrate under catalysis by **M1A** and **M1B** provided similar results after 24 h of reaction (entries 5 and 6, Table 10). In summary, hydrazine was not found to be a better alternative to ammonia borane for the mild and selective reduction of nitroarenes.

### 3. Materials and Methods

#### 3.1. General Remarks

Commercial reagents were used directly as received. Milli-Q water and HPLC grade solvents were used in the preparation and purification of products and nanomaterials. All NMR spectra were recorded with Bruker Avance DRX-250 (250 MHz for <sup>1</sup>H), Bruker Avance DPX-360 MHz (360 MHz for <sup>1</sup>H) and Bruker Avance III 400SB (400 MHz for <sup>1</sup>H) spectrometers (Bruker Biospin, Rheinstetten, Germany). Inductively Coupled Plasma-Optical Emission Spectroscopy (ICP-OES), measurements of metal content were carried out at the *Servei d'Anàlisi Química* of the *Universitat Autònoma de Barcelona* with a Perkin-Elmer instrument, model Optima 4300DV (Perkin-Elmer, Shelton, CT, USA). TEM, ED and

EDS analyses were performed at the *Servei de Microscòpia* of the *Universitat Autònoma de Barcelona*, with a JEOL JEM-2011 model instrument operating at 200 kV (JEOL Ltd, Akishima, Tokyo, Japan). The nanoparticle sizes were determined by measuring 500–1000 particles using ImageJ (Fiji) program and were subsequently averaged to produce the mean NP diameter. XPS measurements were performed with a Phoibos 150 analyzer (SPECS GmbH, Berlin, Germany) in ultra-high vacuum conditions (base pressure 5E-10 mbar) with a monochromatic aluminium K $\alpha$  X-ray source (1486.74 eV); the energy resolution as measured by the FWHM of the Ag 3d $_{5/2}$  peak for a sputtered silver foil was 0.58 eV.

### 3.2. General Procedure for the Preparation of Rh NPs (M1A, Table 1, Entry 1)

Stabilizer **S1A** (43 mg; 0.01 mmol) and rhodium(III) chloride hydrate (135 mg; 0.52 mmol) were dissolved in distilled water (450 mL) under inert atmosphere to afford an orange solution. Then, 50 mL of 0.15 M NaBH $_4$  solution (7.5 mmol) were added dropwise for 10 min and the mixture turned black. The solution was stirred at room temperature overnight. The mixture was filtered through a Milli-Pore filter (0.45  $\mu$ m, nylon) and then extracted with dichloromethane (CH $_2$ Cl $_2$ ) (6  $\times$  30 mL). The organic phase was dried over anhydrous sodium sulfate (Na $_2$ SO $_4$ ), filtered and then the solvent was evaporated to obtain the Rh NPs **M1A** as a black powder (68.2 mg; 31.7% Rh (ICP-OES); 40% yield according to the starting Rh).

### 3.3. General Procedure for the Hydrosilylation of Alkynes by Rh NPs under Neat Conditions (Method A)

To a mixture of alkyne (0.5 mmol) and Rh nanocatalyst (**M1A**, **M1B** or **M2**) (0.5 mol% Rh) into a screw-top sealable tube, triethylsilane (2 mmol) was added. The resulting solution was then heated under stirring at 90  $^{\circ}$ C until total conversion of the alkyne (GC monitoring). Hexane was added to the mixture to precipitate the Rh NPs and the catalyst was separated by centrifugation/decantation. The supernatant was filtered through a plug of silica-gel eluting with hexane and the solvent was removed under an air flow to afford the corresponding vinylsilane.

### 3.4. General Procedure for the Hydrosilylation of Alkynes by Rh NPs in THF (Method B)

A mixture of alkyne (0.5 mmol) and Rh nanocatalyst (**M1A**, **M1B** or **M2**) (0.5 mol% Rh) into a screw-top sealable tube was subjected to three evacuate-refill cycles with argon. Then the corresponding silane (0.6 mmol) and anhydrous and degassed THF (1 mL) were added under argon atmosphere. The reaction mixture was heated under stirring at 90  $^{\circ}$ C until total conversion of the alkyne (Gas chromatography (GC) monitoring). Hexane was added to the mixture to precipitate the Rh NPs and the catalyst was separated by centrifugation/decantation. The supernatant was filtered through a plug of silica-gel eluting with hexane and the solvent was removed under an air flow to afford the corresponding vinylsilane. When the non-volatile triphenylsilane was used, the crude mixture was purified by column chromatography. In the recycling experiments, the Rh nanocatalyst recovered after the centrifugation/decantation process was dried and reused in the next cycle by adding new reagents and solvent in the tube. Spectral data of the vinylsilanes are provided in the Supplementary Materials.

### 3.5. General Procedure for the Reduction of Nitroarenes by Rh NPs with Ammonia Borane

A solution of ammonia borane (2 mmol) in 8 mL of H $_2$ O was added dropwise to a stirred solution of catalyst **M2** (1 mol% Rh) and nitroarene (0.5 mmol) in THF (2 mL) into a sealed tube with an empty balloon to maintain the pressure. Upon completion of the reaction (Thin Layer Chromatography (TLC) monitoring), diethyl ether was added (5 mL), **M2** was maintained in the aqueous phase and the product in the ethereal phase. The two phases were separated by decantation, the aqueous phase was extracted with more diethyl ether (2  $\times$  5 mL). For the recycling of the catalyst the aqueous layer was then extracted with CH $_2$ Cl $_2$  (3  $\times$  5 mL), dried over Na $_2$ SO $_4$  and the solvent was evaporated under reduced pressure to obtain the Rh NPs ready for another cycle. The combined fractions of diethyl ether were washed with water (2  $\times$  5 mL). The organic phase was dried with anhydrous Na $_2$ SO $_4$  and then

the solvent was evaporated under reduced pressure to afford the corresponding pure aniline. Spectral data of the anilines are provided in the Supplementary Materials.

#### 4. Conclusions

In summary, rhodium nanoparticles **M1A**, **M1B** and **M2** have been prepared by reduction of  $\text{RhCl}_3$  with  $\text{NaBH}_4$  in water at room temperature in the presence of the recently reported PEG-tagged imidazolium salts **S1A**, **S1B** and **S2**, respectively. These rhodium nanomaterials are soluble in water and dichloromethane and insoluble in diethyl ether. They have been characterized by TEM, HRTEM, EDS, ED, XPS and ICP-OES.

These Rh NPs **M1A**, **M1B** and **M2** have been successfully used for the stereoselective *syn*-hydrosilylation of symmetric and unsymmetric internal alkynes. The corresponding (*E*)-vinylsilanes were obtained with good yields under two different procedures: (i) solvent-free conditions at 90 °C with an excess of silane; (ii) with THF as solvent with one equivalent of silane at 90 °C in a closed vessel. From low to moderate regioselectivities were achieved, the major regioisomer being the one presenting the silyl group closest to the more electron-withdrawing group. The addition of diethyl ether upon completion of the reaction resulted in the precipitation of the nanocatalyst, which was easily separated from the crude mixture by centrifugation/decantation process. Following this procedure, the nanocatalysts have been recycled up to five runs.

On the other hand, the water-soluble Rh nanocatalysts **M1A**, **M1B** and **M2** have been proved to be effective for the generation of hydrogen from the hydrolysis of ammonia borane (AB). This in situ released hydrogen acted as reductant for the transfer hydrogenation of nitroarenes to the corresponding anilines in THF- $\text{H}_2\text{O}$  1:4 at room temperature. The reaction was successfully carried out with a wide number of nitroaryl compounds bearing different functional groups. The chemoselectivity was not complete when olefin or carbonyl groups were present in the molecule. The Rh NPs were successfully reused up to five cycles.

**Supplementary Materials:** The following are available online at <http://www.mdpi.com/2073-4344/10/10/1195/s1>, Spectral data of the hydrosilylation products. Spectral data of the anilines. Spectra collection.

**Author Contributions:** Conceptualization, R.P.; methodology, G.F.; formal analysis, G.F., and R.P.; writing—original draft preparation, R.P.; writing—review and editing, G.F., and R.P.; supervision, R.P. All authors have read and agreed to the published version of the manuscript.

**Funding:** This research was funded by *Ministerio de Economía, Industria y Competitividad* (MINECO) of Spain, (Projects CTQ2014-53662-P and CTQ2016-81797-REDC), *Ministerio de Ciencia, Innovación y Universidades* (MCINN) of Spain (Project RTI2018-097853-B-I00), *DURSI-Generalitat de Catalunya* (SGR2017-0465).

**Acknowledgments:** We are thankful to *Universitat Autònoma de Barcelona* for predoctoral scholarship to G. F.

**Conflicts of Interest:** The authors declare no conflict of interest. The funders had no role in the design of the study; in the collection, analyses, or interpretation of data; in the writing of the manuscript, or in the decision to publish the results.

#### References

1. Astruc, D. (Ed.) *Nanoparticles and Catalysis*; Wiley-VCH: Weinheim, Germany, 2008; pp. 1–640.
2. Roucoux, A.; Schulz, J.; Patin, H. Reduced Transition Metal Colloids: A Novel Family of Reusable Catalysts? *Chem. Rev.* **2002**, *102*, 3757–3778. [[CrossRef](#)] [[PubMed](#)]
3. Moreno-Mañas, M.; Pleixats, R. Formation of Carbon-Carbon Bonds under Catalysis by Transition-Metal Nanoparticles. *Acc. Chem. Res.* **2003**, *36*, 638–643. [[CrossRef](#)] [[PubMed](#)]
4. Widgren, J.A.; Finke, R.G. A review of soluble transition-metal nanoclusters as arene hydrogenation catalysts. *J. Mol. Catal. A Chem.* **2003**, *191*, 187–207. [[CrossRef](#)]
5. Astruc, D.; Lu, F.; Ruiz Aranzaes, J. Nanoparticles as recyclable catalysts: The frontier between homogeneous and heterogeneous catalysis. *Angew. Chem. Int. Ed.* **2005**, *44*, 7852–7872. [[CrossRef](#)]
6. De Vries, J.G. A unifying mechanism for all high-temperature Heck reactions. The role of palladium colloids and anionic species. *Dalton Trans.* **2006**, 421–429. [[CrossRef](#)]

7. Astruc, D. Palladium nanoparticles as efficient green homogeneous and heterogeneous carbon-carbon coupling precatalysts: A unifying view. *Inorg. Chem.* **2007**, *46*, 1884–1894. [[CrossRef](#)]
8. Roucoux, A.; Philippot, K. Homogeneous Hydrogenation. Colloids. Hydrogenation with Noble Metal Nanoparticles. In *Handbook of Homogeneous Hydrogenation*; De Vries, J.G., Elsevier, C.J., Eds.; Wiley-VCH: Weinheim, Germany, 2007; Volume 9, pp. 217–255.
9. Corma, A.; García, H. Supported gold nanoparticles as catalysts for organic reactions. *Chem. Rev.* **2008**, *37*, 2096–2126. [[CrossRef](#)]
10. Roy, S.; Pericàs, M.A. Functionalized nanoparticles as catalysts for enantioselective processes. *Org. Biomol. Chem.* **2009**, *7*, 2669–2677. [[CrossRef](#)]
11. Starkey Ott, L.; Finke, R.G. Transition-metal nanocluster stabilization for catalysis: A critical review of ranking methods and putative stabilizers. *Coord. Chem. Rev.* **2007**, *251*, 1075–1100.
12. Guerrero, M.; Than Chau, N.T.; Noël, S.; Denicourt-Nowicki, A.; Hapiot, F.; Roucoux, A.; Monflier, E.; Philippot, K. About the Use of Rhodium Nanoparticles in Hydrogenation and Hydroformylation Reactions. *Curr. Org. Chem.* **2013**, *17*, 364–399. [[CrossRef](#)]
13. Roucoux, A.; Nowicki, A.; Philippot, K. Rhodium and Ruthenium Nanoparticles in Catalysis. In *Nanoparticles and Catalysis*; Astruc, D., Ed.; Wiley-VCH: Weinheim, Germany, 2008; pp. 349–388, Chapter 11.
14. Yuan, Y.; Yan, N.; Dyson, P.J. Advances in the Rational Design of Rhodium Nanoparticle Catalysts: Control via Manipulation of the Nanoparticle Core and Stabilizer. *ACS Catal.* **2012**, *2*, 1057–1069. [[CrossRef](#)]
15. Kadam, H.K.; Tilve, S.G. Advancements in methodologies for reduction of nitroarenes. *RSC Adv.* **2015**, *5*, 83391–83407. [[CrossRef](#)]
16. Zhao, P.; Feng, X.; Huang, D.; Yang, G.; Astruc, D. Basic concepts and recent advances in nitrophenol reduction by gold- and other transition metal nanoparticles. *Coord. Chem. Rev.* **2015**, *287*, 114–136. [[CrossRef](#)]
17. Aditya, T.; Pal, A.; Pal, T. Nitroarene reduction: A trusted model reaction to test nanoparticle catalysts. *Chem. Commun.* **2015**, *51*, 9410–9431. [[CrossRef](#)] [[PubMed](#)]
18. Serna, P.; Corma, A. Transforming Nano Metal Nonselective Particulates into Chemoselective Catalysts for Hydrogenation of Substituted Nitrobenzenes. *ACS Catal.* **2015**, *5*, 7114–7121. [[CrossRef](#)]
19. Nakamura, I.; Yamanoi, Y.; Yonezawa, T.; Imaoka, T.; Yamamoto, K.; Nishihara, H. Nanocage catalysts-rhodium nanoclusters encapsulated with dendrimers as accessible and stable catalysts for olefin and nitroarene hydrogenations. *Chem. Commun.* **2008**, 5716–5718. [[CrossRef](#)]
20. Nakamura, I.; Yamanoi, Y.; Imaoka, T.; Yamamoto, K.; Nishihara, H. A Uniform Bimetallic Rhodium/Iron Nanoparticle Catalyst for the Hydrogenation of Olefins and Nitroarenes. *Angew. Chem. Int. Ed.* **2011**, *50*, 5830–5833. [[CrossRef](#)]
21. Corma, A.; Serna, P. Chemoselective Hydrogenation of Nitro Compounds with Supported Gold Catalysts. *Science* **2006**, *313*, 332–334. [[CrossRef](#)]
22. Chen, Y.; Qiu, J.; Wang, X.; Xiu, J. Preparation and application of highly dispersed gold nanoparticles supported on silica for catalytic hydrogenation of aromatic nitro compounds. *J. Catal.* **2006**, *242*, 227–230. [[CrossRef](#)]
23. Lara, P.; Suárez, A.; Collière, V.; Philippot, K.; Chaudret, B. Platinum N-Heterocyclic Carbene Nanoparticles as New and Effective Catalysts for the Selective Hydrogenation of Nitroaromatics. *ChemCatChem* **2014**, *6*, 87–90. [[CrossRef](#)]
24. Lara, P.; Philippot, K. The hydrogenation of nitroarenes mediated by platinum nanoparticles: An overview. *Catal. Sci. Technol.* **2014**, *4*, 2445–2465. [[CrossRef](#)]
25. Wu, H.; Zhuo, L.; He, Q.; Liao, X.; Shi, B. Heterogeneous hydrogenation of nitrobenzenes over recyclable Pd(0) nanoparticles catalysts stabilized by polyphenol-grafted collagen fibers. *Appl. Catal. A Gen.* **2009**, *366*, 44–56. [[CrossRef](#)]
26. Li, J.; Shi, X.-Y.; Bi, Y.-Y.; Wei, J.-F.; Chen, Z.-G. Pd Nanoparticles in Ionic Liquid Brush: A Highly Active and Reusable Heterogeneous Catalytic Assembly for Solvent-Free or On-Water Hydrogenation of Nitroarene under Mild Conditions. *ACS Catal.* **2011**, *1*, 657–664. [[CrossRef](#)]
27. Liu, W.-J.; Tian, K.; Jiang, H. One-pot synthesis of Ni-NiFe<sub>2</sub>O<sub>4</sub>/carbon nanofiber composites from biomass for selective hydrogenation of aromatic nitro compounds. *Green Chem.* **2015**, *17*, 821–826. [[CrossRef](#)]
28. Pisiewicz, S.; Formenti, D.; Surkus, A.-E.; Pohl, M.-M.; Radnik, J.; Junge, K.; Topf, C.; Bachmann, S.; Scalone, M.; Beller, M. Synthesis of Nickel Nanoparticles with N-Doped Graphene Shells for Catalytic Reduction Reactions. *ChemCatChem* **2016**, *8*, 129–134. [[CrossRef](#)]

29. Huang, L.; Luo, P.; Pei, X.; Liu, X.; Wang, Y.; Wang, J.; Xing, W.; Huang, J. Selective Hydrogenation of Nitroarenes and Olefins over Rhodium Nanoparticles on Hydroxyapatite. *Adv. Synth. Catal.* **2012**, *354*, 2689–2694. [[CrossRef](#)]
30. Luo, P.; Xu, K.; Zhang, R.; Huang, L.; Wang, J.; Xing, W.; Huang, J. Highly efficient and selective reduction of nitroarenes with hydrazine over supported rhodium nanoparticles. *Catal. Sci. Technol.* **2012**, *2*, 301–304. [[CrossRef](#)]
31. Ganji, S.; Sankar Enumula, S.; Kumar Marella, R.; Seetha Rama Rao, K.; Raju Burri, D. RhNPs/SBA-NH<sub>2</sub>: A high-performance catalyst for aqueous phase reduction of nitroarenes to aminoarenes at room temperature. *Catal. Sci. Technol.* **2014**, *4*, 1813–1819. [[CrossRef](#)]
32. Zhou, J.; Li, Y.; Sun, H.-B.; Tang, Z.; Qi, L.; Liu, L.; Ai, Y.; Li, S.; Shao, Z.; Liang, Q. Porous silica-encapsulated and magnetically recoverable Rh NPs: A highly efficient, stable and green catalyst for catalytic transfer hydrogenation with “slow-release” of stoichiometric hydrazine in water. *Green Chem.* **2017**, *19*, 3400–3407. [[CrossRef](#)]
33. Guo, W.; Pleixats, R.; Shafir, A. Water-Soluble Gold Nanoparticles: From Catalytic Selective Nitroarene Reduction in Water to Refractive Index Sensing. *Chem. Asian J.* **2015**, *10*, 2437–2443. [[CrossRef](#)]
34. Fernández, G.; Sort, J.; Pleixats, R. Nickel Nanoparticles Stabilized by Tris-imidazolium Salts: Synthesis, Characterization and Application as Recyclable Catalysts for the Reduction of Nitroarenes. *ChemistrySelect* **2018**, *3*, 8597–8603. [[CrossRef](#)]
35. Trost, B.M.; Ball, Z.T.; Töge, T. A Chemoselective Reduction of Alkynes to (E)-Alkenes. *J. Am. Chem. Soc.* **2002**, *124*, 7922–7923. [[CrossRef](#)] [[PubMed](#)]
36. May, T.L.; Dabrowski, J.A.; Hoveyda, A.H. Formation of vinyl-, vinylhalide- or acyl-substituted quaternary carbon stereogenic centers through NHC-Cu-catalyzed enantioselective conjugate additions of Si-containing vinylaluminums to  $\beta$ -substituted cyclic enones. *J. Am. Chem. Soc.* **2011**, *133*, 736–739. [[CrossRef](#)]
37. Jones, G.R.; Landais, Y. The oxidation of the carbon-silicon bond. *Tetrahedron* **1996**, *52*, 7599–7662. [[CrossRef](#)]
38. Nakao, Y.; Hiyama, T. Silicon-based cross-coupling reaction: An environmentally benign version. *Chem. Soc. Rev.* **2011**, *40*, 4893–4901. [[CrossRef](#)] [[PubMed](#)]
39. Marciniak, B. Catalysis of hydrosilylation of carbon-carbon multiple bonds: Recent progress. *Silicon Chem.* **2002**, *1*, 155–174. [[CrossRef](#)]
40. Marciniak, B.; Maciejewski, H.; Pietraszuk, C.; Pawluc, P. Hydrosilylation of Alkynes and Their Derivatives. In *Hydrosilylation: A Comprehensive Review on Recent Advances (Advances in Silicon Science Series)*; Marciniak, B., Ed.; Springer: Berlin, Germany, 2009; Volume 1, Chapter 2.
41. Bali, Z.T. C-E Bond Formation through Hydrosilylation of Alkynes and Related Reactions. In *Comprehensive Organometallic Chemistry III*; Mingos, D.M.P., Crabtree, R.H., Eds.; Elsevier Ltd.: Oxford, UK, 2007; Volume 10, pp. 789–813.
42. Dierick, S.; Markó, I.E. NHC Platinum(0) Complexes: Unique Catalysts for the Hydrosilylation of Alkenes and Alkynes. In *N-Heterocyclic Carbenes: Effective Tools for Organometallic Synthesis*; Nolan, S.P., Ed.; Wiley-VCH: Weinheim, Germany, 2014; pp. 111–149, Chapter 5.
43. Sun, J.; Deng, L. Cobalt Complex-Catalyzed Hydrosilylation of Alkenes and Alkynes. *ACS Catal.* **2016**, *6*, 290–300. [[CrossRef](#)]
44. Zaranek, M.; Marciniak, B.; Pawluc, P. Ruthenium-catalyzed hydrosilylation of carbon-carbon multiple bonds. *Org. Chem. Front.* **2016**, *3*, 1337–1344. [[CrossRef](#)]
45. Sanada, T.; Kato, T.; Mitani, M.; Mori, A. Rhodium-Catalyzed Hydrosilylation of Internal Alkynes with Silane Reagents bearing Heteroatom Substituents. Studies on the Regio-/Stereochemistry and Transformation of the Produced Alkenylsilanes by Rhodium-Catalyzed Conjugate Addition. *Adv. Synth. Catal.* **2006**, *348*, 51–54. [[CrossRef](#)]
46. Field, L.D.; Ward, A.J. Catalytic hydrosilylation of acetylenes mediated by phosphine complexes of cobalt(I), rhodium(I), and iridium(I). *J. Organomet. Chem.* **2003**, *681*, 91–97. [[CrossRef](#)]
47. Sato, A.; Kinoshita, H.; Shinokubo, H.; Oshima, K. Hydrosilylation of Alkynes with a Cationic Rhodium Species Formed in an Anionic Micellar System. *Org. Lett.* **2004**, *6*, 2217–2220. [[CrossRef](#)]
48. Nagashima, H.; Tatebe, K.; Ishibashi, T.; Sakakibara, J.; Itoh, K. (PPh<sub>3</sub>)<sub>3</sub>RhCl-catalyzed hydrosilylation of unsaturated molecules by 1,2-bis(dimethylsilyl)ethane: Unprecedented rate difference between two silicon-hydrogen bonds. *Organometallics* **1989**, *8*, 2495–2496. [[CrossRef](#)]

49. Cassani, M.C.; Brucka, M.A.; Femoni, C.; Mancinelli, M.; Mazzanti, A.; Mazzoni, R.; Solinas, G. *N*-Heterocyclic carbene rhodium(I) complexes containing an axis of chirality: Dynamics and catalysis. *N. J. Chem.* **2014**, *38*, 1768–1779. [[CrossRef](#)]
50. Rivera, G.; Elizalde, O.; Roa, G.; Montiel, I.; Bernès, S. Fluorinated *N*-heterocyclic carbenes rhodium(I) complexes and their activity in hydrosilylation of propargylic alcohols. *J. Organomet. Chem.* **2012**, *699*, 82–86. [[CrossRef](#)]
51. Solomonsz, W.A.; Rance, G.A.; Khlobystov, A.N. Evaluating the Effects of Carbon Nanoreactor Diameter and Internal Structure on the Pathways of the Catalytic Hydrosilylation Reaction. *Small* **2014**, *10*, 1866–1872. [[CrossRef](#)] [[PubMed](#)]
52. Alonso, F.; Buitrago, R.; Moglie, Y.; Ruiz-Martínez, J.; Sepúlveda-Escribano, A.; Yus, M. Hydrosilylation of alkynes catalysed by platinum on titania. *J. Organomet. Chem.* **2011**, *696*, 368–372. [[CrossRef](#)]
53. Alonso, F.; Buitrago, R.; Moglie, Y.; Sepúlveda-Escribano, A.; Yus, M. Selective Hydrosilylation of 1,3-Diynes Catalyzed by Titania-Supported Platinum. *Organometallics* **2012**, *31*, 2336–2342. [[CrossRef](#)]
54. Cano, R.; Yus, M.; Ramón, D.J. Impregnated Platinum on Magnetite as an Efficient, Fast, and Recyclable Catalyst for the Hydrosilylation of Alkynes. *ACS Catal.* **2012**, *2*, 1070–1078. [[CrossRef](#)]
55. Solomonsz, W.A.; Rance, G.A.; Harris, B.J.; Khlobystov, A.N. Competitive hydrosilylation in carbon nanoreactors: Probing the effect of nanoscale confinement on selectivity. *Nanoscale* **2013**, *5*, 12200–12205. [[CrossRef](#)]
56. Hu, W.; Xie, H.; Yue, H.; Prinsen, P.; Luque, R. Super-microporous silica-supported platinum catalyst for highly regioselective hydrosilylation. *Catal. Commun.* **2017**, *97*, 51–55. [[CrossRef](#)]
57. Rivero-Crespo, M.A.; Leyva-Pérez, A.; Corma, A. A Ligand-Free Pt<sub>3</sub> Cluster Catalyzes the Markovnikov Hydrosilylation of Alkynes with up to 10<sup>6</sup> Turnover Frequencies. *Chem. Eur. J.* **2017**, *23*, 1702–1708. [[CrossRef](#)] [[PubMed](#)]
58. Chauhan, B.P.S.; Sarkar, A. Functionalized vinylsilanes via highly efficient and recyclable Pt-nanoparticle catalysed hydrosilylation of alkynes. *Dalton Trans.* **2017**, *46*, 8709–8715. [[CrossRef](#)] [[PubMed](#)]
59. Duke, B.J.; Akeroyd, E.N.; Bhatt, S.V.; Onyeagusi, C.I.; Bhatt, S.V.; Adolph, B.R.; Fotie, J. Nano-dispersed platinum(0) in organically modified silicate matrices as sustainable catalysts for a regioselective hydrosilylation of alkenes and alkynes. *N. J. Chem.* **2018**, *42*, 11782–11795. [[CrossRef](#)]
60. Fernández, G.; Pleixats, R. Soluble Pt Nanoparticles Stabilized by a Tris-Imidazolium Tetrafluoroborate as Efficient and Recyclable Catalyst for the Stereoselective Hydrosilylation of Alkynes. *ChemistrySelect* **2018**, *3*, 11486–11493. [[CrossRef](#)]
61. Planellas, M.; Guo, W.; Alonso, F.; Yus, M.; Shafir, A.; Pleixats, R.; Parella, T. Hydrosilylation of Internal Alkynes Catalyzed by Tris-Imidazolium Salt-Stabilized Palladium Nanoparticles. *Adv. Synth. Catal.* **2014**, *356*, 179–188. [[CrossRef](#)]
62. Duan, Y.; Ji, G.; Zhang, S.; Chen, X.; Yang, Y. Additive-modulated switchable reaction pathway in the addition of alkynes with organosilanes catalyzed by supported Pd nanoparticles: Hydrosilylation versus semihydrogenation. *Cat. Sci. Technol.* **2018**, *8*, 1039–1050. [[CrossRef](#)]
63. Solomonsz, W.A.; Rance, G.A.; Suyetin, M.; La Torre, A.; Bichoutskaia, E.; Khlobystov, A.N. Controlling the Regioselectivity of the Hydrosilylation Reaction in Carbon Nanoreactors. *Chem. Eur. J.* **2012**, *18*, 13180–13187. [[CrossRef](#)]
64. Psyllaki, A.; Lykakis, I.N.; Stratakis, M. Reaction of hydrosilanes with alkynes catalyzed by gold nanoparticles supported on TiO<sub>2</sub>. *Tetrahedron* **2012**, *68*, 8724–8731. [[CrossRef](#)]
65. Ishikawa, Y.; Yamamoto, Y.; Asao, N. Selective hydrosilylation of alkynes with a nanoporous gold catalyst. *Catal. Sci. Technol.* **2013**, *3*, 2902–2905. [[CrossRef](#)]
66. Guo, W.; Pleixats, R.; Shafir, A.; Parella, T. Rhodium Nanoflowers Stabilized by a Nitrogen-Rich PEG-Tagged Substrate as Recyclable Catalyst for the Stereoselective Hydrosilylation of Internal Alkynes. *Adv. Synth. Catal.* **2015**, *357*, 89–99. [[CrossRef](#)]
67. Fernández, G.; Bernardo, L.; Villanueva, A.; Pleixats, R. Gold nanoparticles stabilized by PEG-tagged imidazolium salts as recyclable catalysts for the synthesis of propargylamines and the cycloisomerization of  $\gamma$ -alkynoic Acids. *N. J. Chem.* **2020**, *44*, 6130–6141. [[CrossRef](#)]
68. Yao, Q.; Lu, Z.-H.; Jia, Y.; Chen, X.; Liu, X. In situ facile synthesis of Rh nanoparticles supported on carbon nanotubes as highly active catalysts for H<sub>2</sub> generation from NH<sub>3</sub>BH<sub>3</sub> hydrolysis. *Int. J. Hydrogen Energy* **2015**, *40*, 2207–2215. [[CrossRef](#)]

69. Gopiraman, M.; Saravanamoorthy, S.; Ullah, S.; Ilangovan, A.; Kim, I.S.; Chung, I.M. Reducing-agent-free facile preparation of Rh nanoparticles uniformly anchored on onion-like fullerene for catalytic applications. *RSC Adv.* **2020**, *10*, 2545–2559. [[CrossRef](#)]
70. Liu, C.; Zhang, J.; Liu, H.; Qiu, J.; Zhang, X. Heterogeneous Ligand-Free Rhodium Oxide Catalyst Embedded within Zeolitic Microchannel to Enhance Regioselectivity in Hydroformylation. *Ind. Eng. Chem. Res.* **2019**, *58*, 21285–21295. [[CrossRef](#)]
71. Zahmakiran, M.; Özkar, S. Transition Metal Nanoparticles in Catalysis for the Hydrogen Generation from the Hydrolysis of Ammonia-Borane. *Top. Catal.* **2013**, *56*, 1171–1183. [[CrossRef](#)]
72. Zhao, T.-J.; Zhang, Y.-N.; Wang, K.-X.; Su, J.; Wei, X.; Li, X.-H. General transfer hydrogenation by activating ammonia-borane over cobalt nanoparticles. *RSC Adv.* **2015**, *5*, 102736–102740. [[CrossRef](#)]
73. Wang, W.; Ciganda, R.; Wang, C.; Escobar, A.; Martínez-Villacorta, A.M.; Ramírez, M.A.; Hernández, R.; Moya, S.E.; Ruiz, J.; Hamon, J.-R.; et al. High catalytic activity of Rh nanoparticles generated from cobaltocene and RhCl<sub>3</sub> in aqueous solution. *Inorg. Chem. Front.* **2019**, *6*, 2704–2708. [[CrossRef](#)]
74. Akbayrak, S.; Tonbul, Y.; Özkar, S. Magnetically Separable Rh<sub>0</sub>/Co<sub>3</sub>O<sub>4</sub> Nanocatalyst Provides over a Million Turnovers in Hydrogen Release from Ammonia Borane. *ACS Sustain. Chem. Eng.* **2020**, *8*, 4216–4224. [[CrossRef](#)]
75. Luo, W.; Zhao, X.; Cheng, W.; Zhang, Y.; Wang, Y.; Fan, G. A simple and straightforward strategy for synthesis of N, P co-doped porous carbon: An efficient support for Rh nanoparticles for dehydrogenation of ammonia borane and catalytic application. *Nanoscale Adv.* **2020**, *2*, 1685–1693. [[CrossRef](#)]

**Publisher's Note:** MDPI stays neutral with regard to jurisdictional claims in published maps and institutional affiliations.



© 2020 by the authors. Licensee MDPI, Basel, Switzerland. This article is an open access article distributed under the terms and conditions of the Creative Commons Attribution (CC BY) license (<http://creativecommons.org/licenses/by/4.0/>).